

























































These values must be converted from their absolute form (which is subject to performance variations) to a form which is valid for all actuator instances. This can be done by expressing the value as a percentage change from the fault-free average, or as a simple difference from the fault-free average. These conversions are the weak point of such an algorithm, but the results suggest that they are sufficient to get quite a positive response from a diagnosis system.

## 5.4 The resulting system

The result of the considerations described in the previous sections is a functional design for a system which uses the minimal data set and the data from each monitored throw of an actuator to calculate a confidence level for the presence of each fault.

Figure 14 shows the first level functionality of this system. Function 1 is performed once, when all the fault simulations have been completed. It performs QTA on the data, finds the common episodes and establishes rules on the values connected with those episodes.

Function 2 is performed every time the diagnosis system is installed on an actuator. The data from the actuator's "running-in" are used to find a baseline for performance. QTA is performed on the data and the absolute values connected with the common episodes are stored. When the actuator is in operation, QTA is performed on the measured data by function 3, and the values are converted into relative quantities using the fault free absolute values found by function 2. A subtractive method (as specified in equation (1), where  $V_{rel}$  is the relative value for the current operation,  $V_{ff}$  is the fault-free absolute value and  $V_{op}$  is the absolute value measured during the current operation) was the most effective approach attempted.

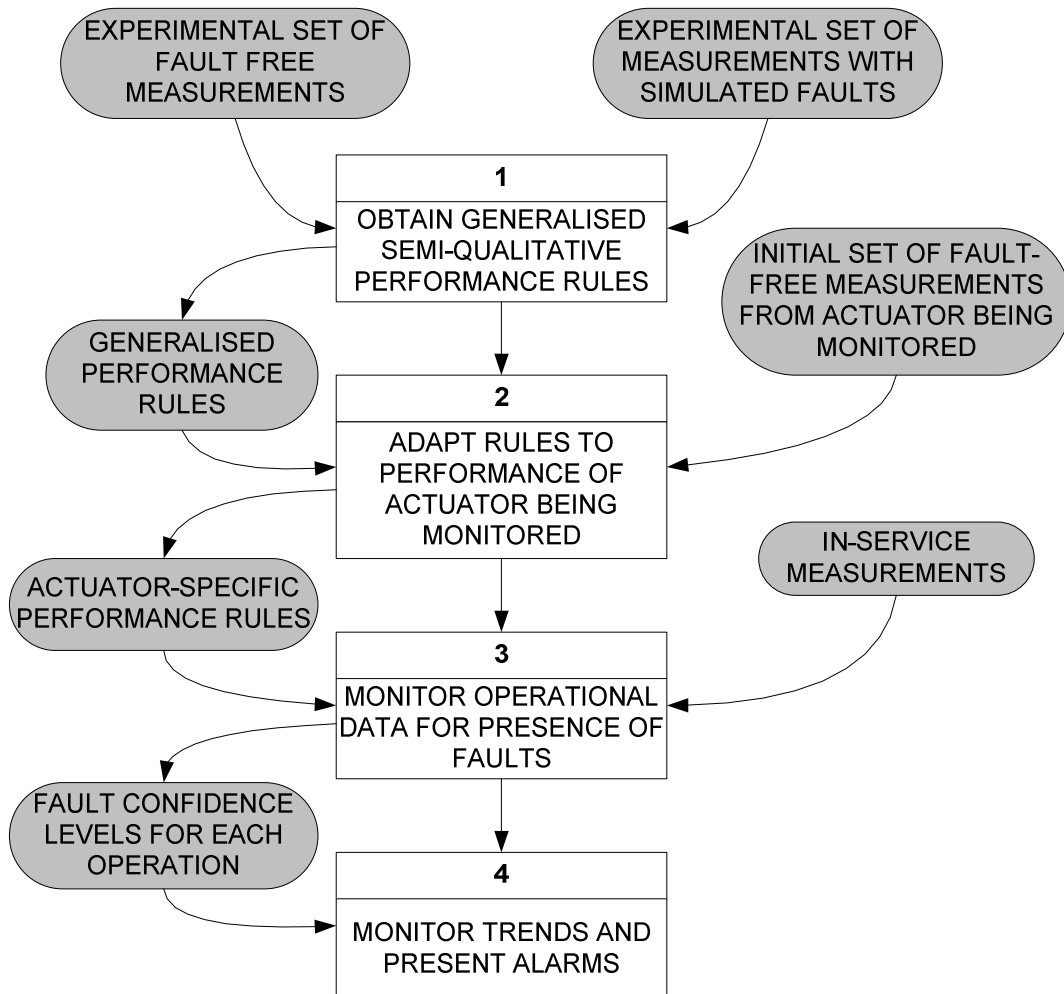
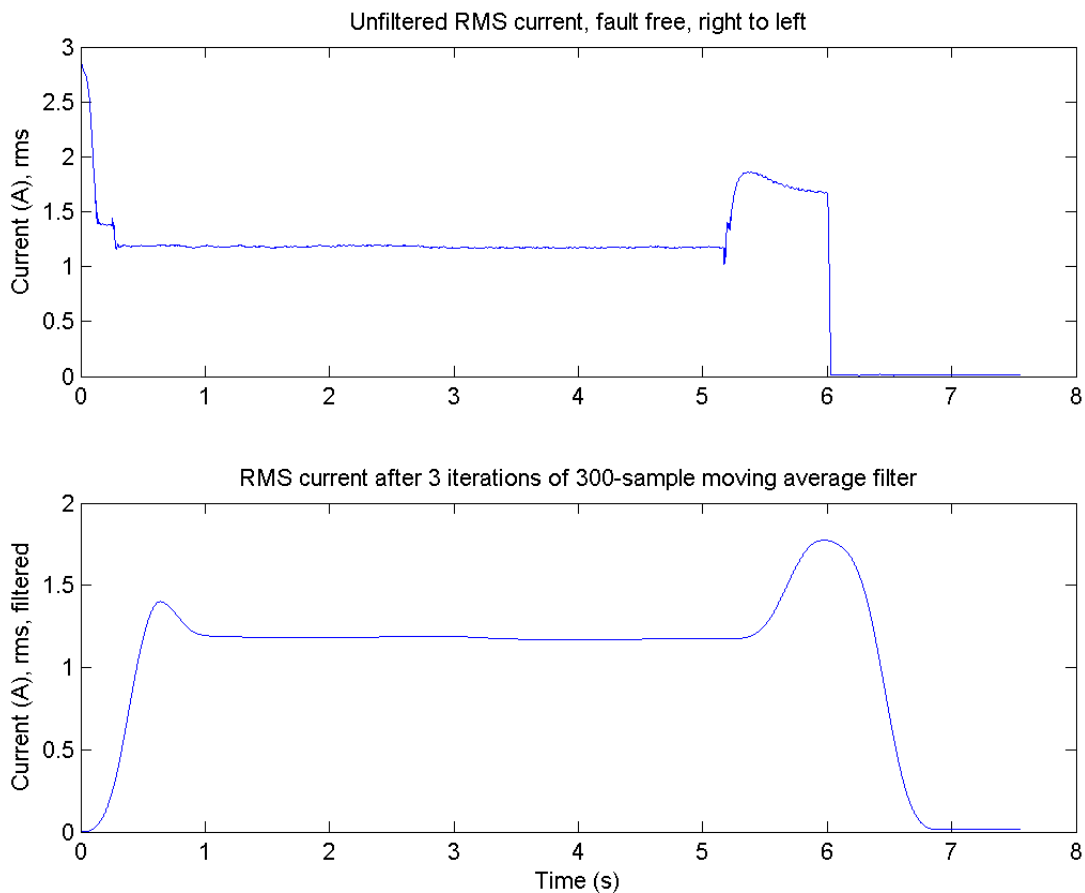


Figure 14 - EFFBD showing level 1 of the proposed system

$$V_{rel} = V_{op} - V_{ff} \tag{1}$$

One important point to note is that the QTA method is sensitive to the scale of the trends it must analyse. Unfiltered data contains too many turning points to effectively isolate the trends of interest. For this reason, the data are filtered using an approximation of the Gaussian filter, implemented by successive applications of a local-averaging filter (a rectangular filtering function). This eliminates the high-frequency data, leaving a waveform which is a smooth set of curves which are consistent from one waveform to the next.

Figure 15 illustrates the effects of this filtering method. It may seem a little drastic, but the important trends will be affected in the same way by faults when viewed in the filtered waveform – but now, the system is not distracted by the smaller variations which mean less in terms of fault effects.



**Figure 15 - Comparison of unfiltered and filtered waveforms**

## 5.5 QTA and rule base construction in detail

Figure 14 shows the top level of the system’s functionality. This section will now focus on the contents of function 1 in that diagram. The establishment of the rule base is carried out in two stages, the first being a QTA of the test data set, as already mentioned. Figure 16 shows the lower-level functional flow of the QTA process.

The differentiated values (gradients) of the waveform are used in the process of classifying partitions. By comparing the starting gradient with the ending gradient for a partition, it is possible to determine what shape the curve is, between the two points. The partitioning interval is chosen such that it is smaller than the dynamics of the waveform, thereby preventing the system from missing important trends.

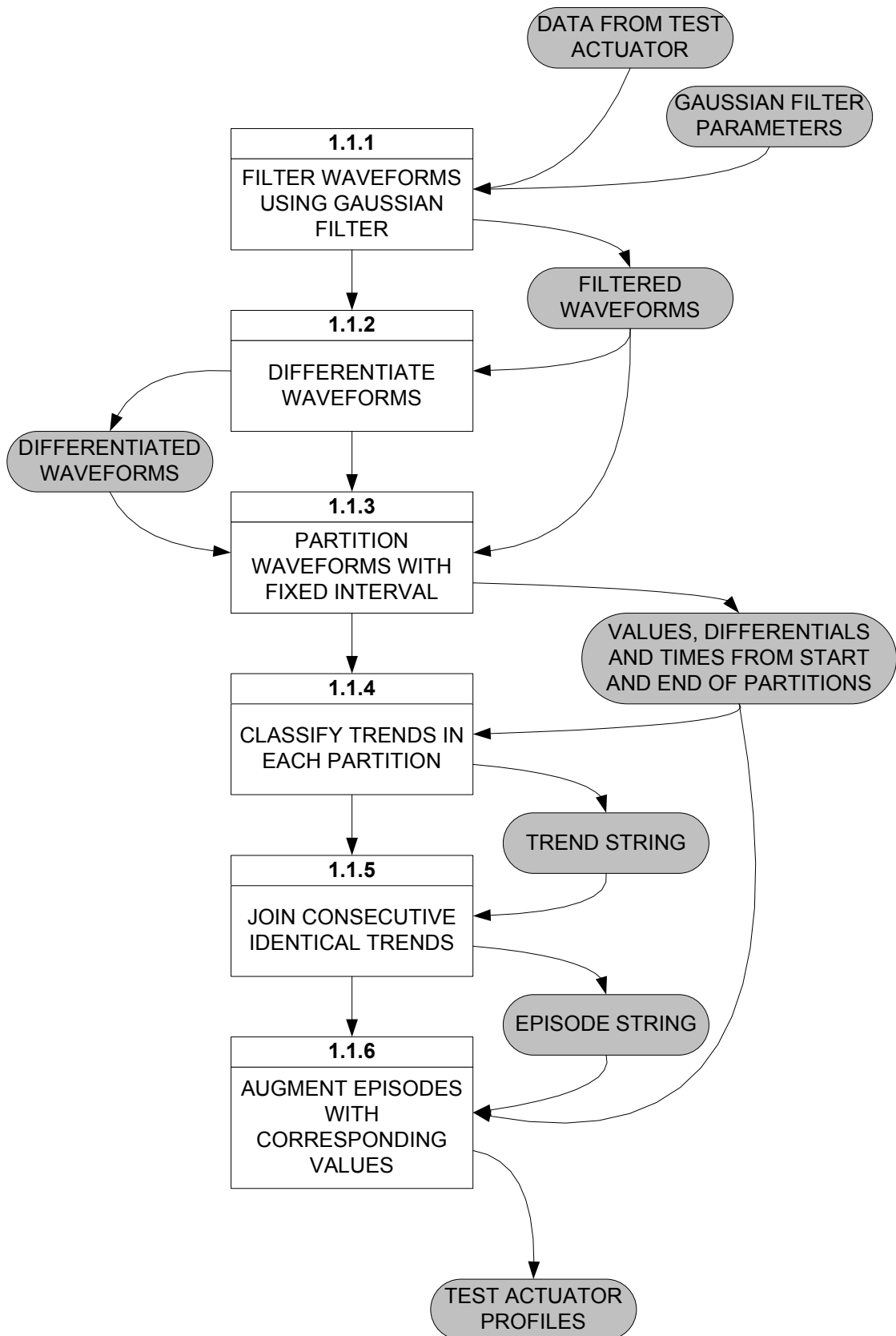


**Figure 16 - EFFBD illustrating the process of QTA for the establishment of rules**

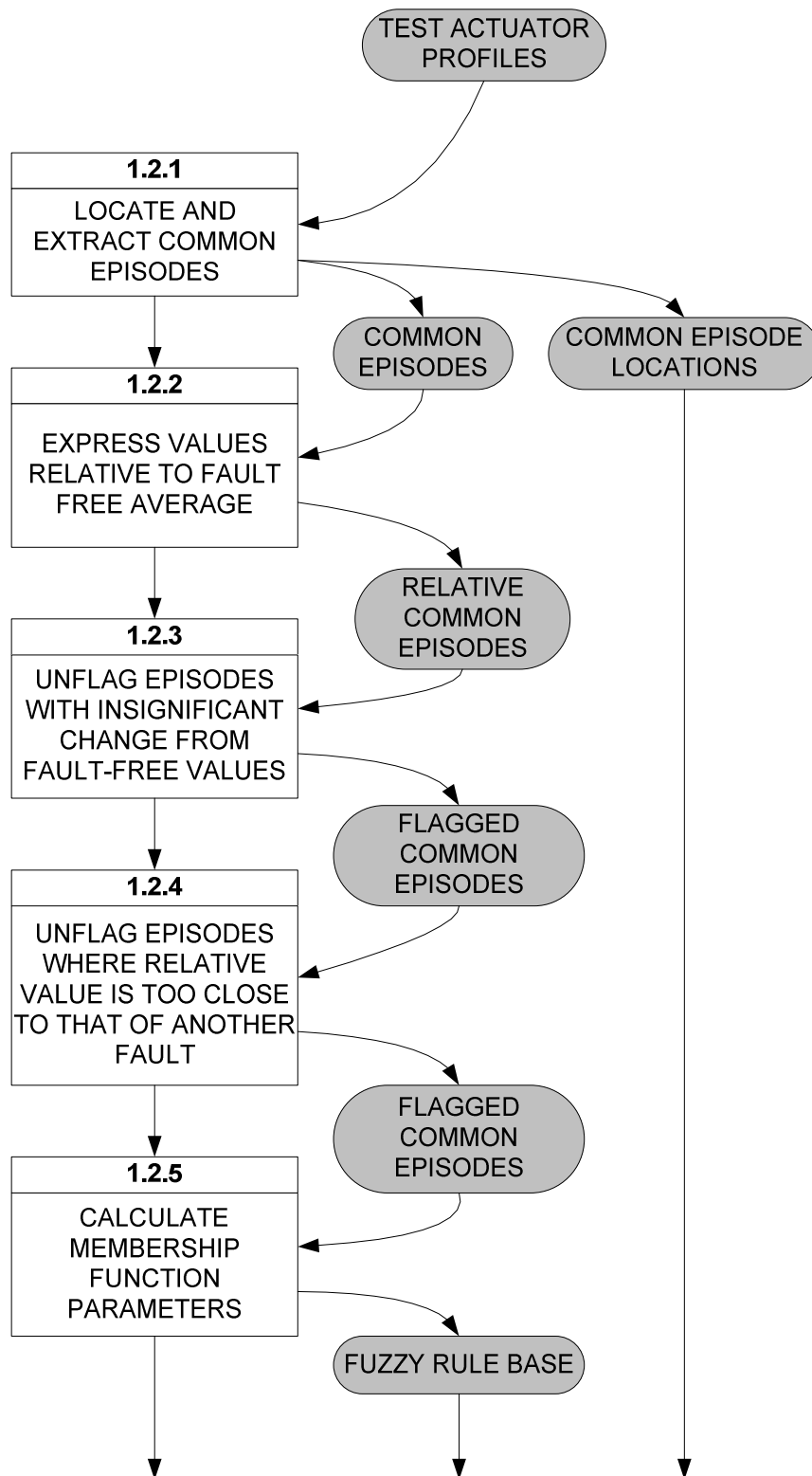


Figure 17 - EFFBD illustrating the formation of rules

The trend string consists of the qualitative states for each partition (i.e. the shape classification, written as a letter between A and I), the values of each filtered waveform at the start and end of the partition, and the time coordinates of the start and end of the partition.

When the trend string contains more than one partition which has the same shape, these are joined to form *episodes*. The episodes have the same format as the trends: containing qualitative state, start time, end time and the start and end values of the waveform. The episodes which make up a single waveform are called a *profile*.

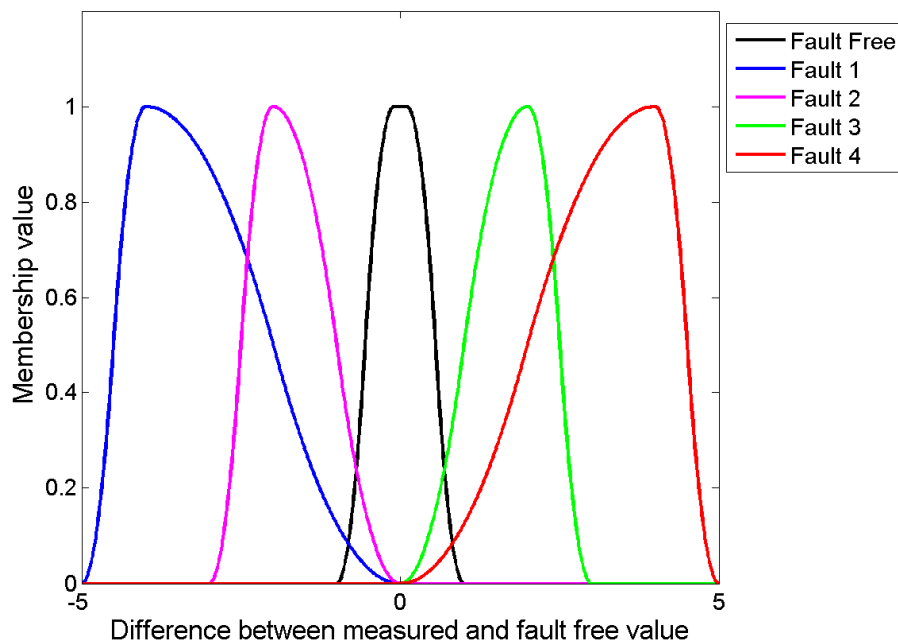
The QTA is carried out separately for each variable measured.

Once a profile has been generated for each waveform in the test data set, the rules can be established. This process is illustrated in Figure 17. First, it is necessary to find the episodes which are common throughout the data set. This is important because the values in the episodes are compared to the values in the fault free set. This can only be done with episodes which are always present in the waveforms.

The values for each common episode are then converted from the absolute representation into a relative representation by taking the difference between the current value and the average value, for the same episode, under fault free conditions. A flag is added initially to each such value, signifying that it is suitable for rule formation.

Flags are then removed if the relative values are too small (i.e. too close to fault-free) and if they are too close to the relative value, for the same episode, from a different fault condition. These unflagging processes make the system stronger at diagnosing faults and at differentiating between them.

For each relative value which is still flagged, a fuzzy rule is created. Fuzzy rules represent the gradual transition from fault-free to faulty with a membership function which changes slowly from 0 to 1 as the fault becomes stronger.



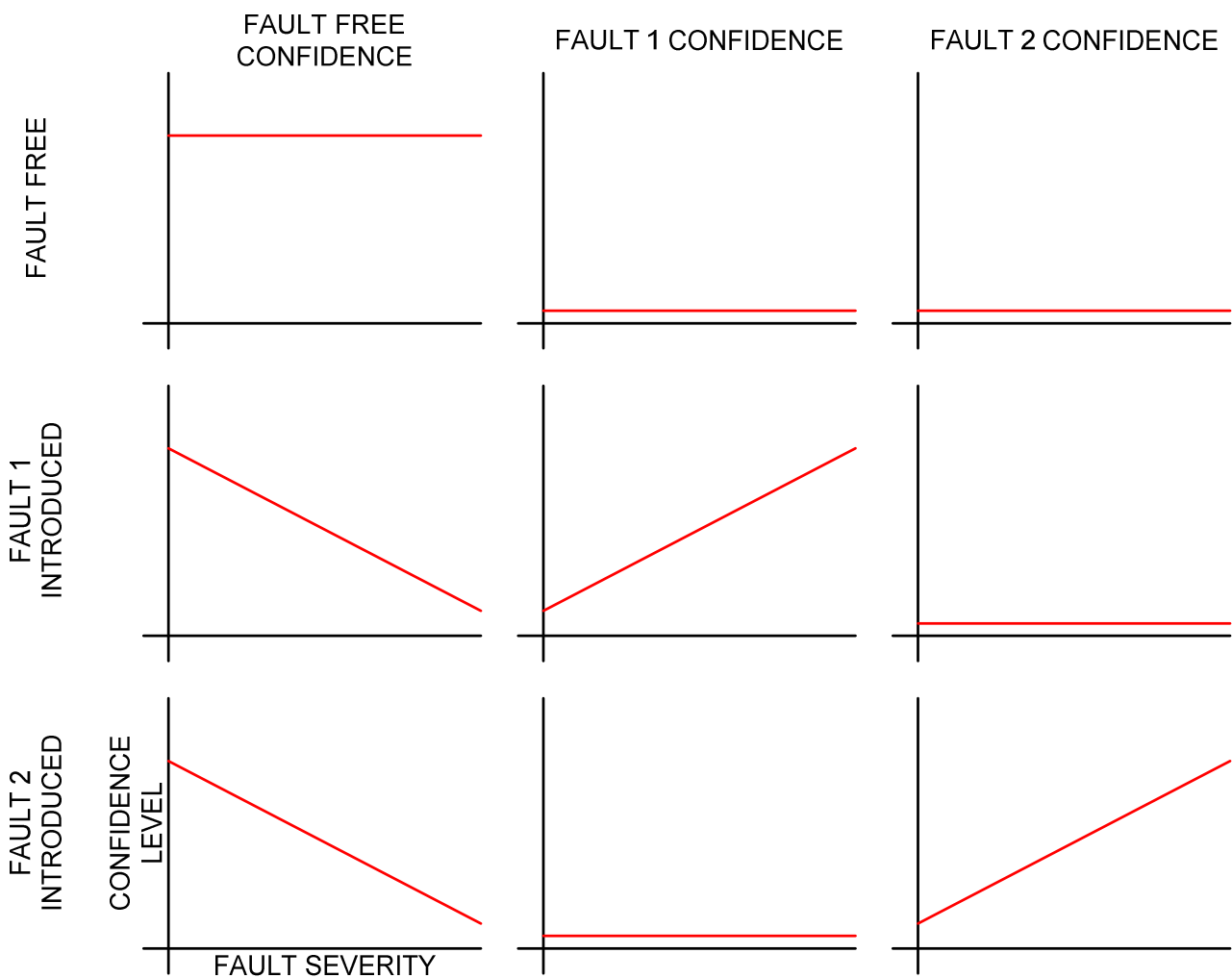
**Figure 18 –  $\Pi$ -shaped membership functions**

Figure 18 shows an example rule set for one particular quantity. The  $x$ -axis here is the straight difference between the current measured value and the fault-free average. Each fault condition has a membership function whose peak is at the value which was measured during fault simulation. If each fault is simulated to a point where any further adjustments cause the monitored asset to fail, then we can impose a decline in the membership function, once the peak value has been reached: we know that if this fault were present, the actuator would be about to fail – so if the variation continues to get further from fault-free, we know that this fault is not to blame, because it would have stopped the actuator from working.

By forming a number of these rules, working with different episodes in the waveform and different measured variables, a very strong diagnosis system can be built, impervious to the variations between machines and able to tell the difference between a wide range of faults, based on the changes to individual episodes in the measured data.

## 5.6 Diagnosis of faults

When the monitored actuator is in service, the key parameters are measured each time it operates. This produces waveforms which are subject to the same QTA as previously described. Function 3, the diagnosis function, finds the common episodes each time, and uses their relative values to evaluate the membership functions for each rule. The average membership is taken for the rules pertaining to each fault, producing a confidence level for each fault, for that operation. Over time, an increase in a fault's confidence value indicates that the presence of that fault is becoming more likely.



**Figure 19 - Ideal output of the fault diagnosis system**

Figure 19 shows the ideal output of the fault diagnosis system. Each row of graphs shows the confidence level for each possible fault, under the same simulated condition. The first row is the control. Subsequent rows show how the fault confidence level changes as a fault is introduced. Looking at row 2, the confidence level for the fault-free condition reduces as the fault increases in severity. Conversely, the confidence level for fault 1 increases. The confidence level for fault 2 remains very small, because that fault is not currently present in the actuator.

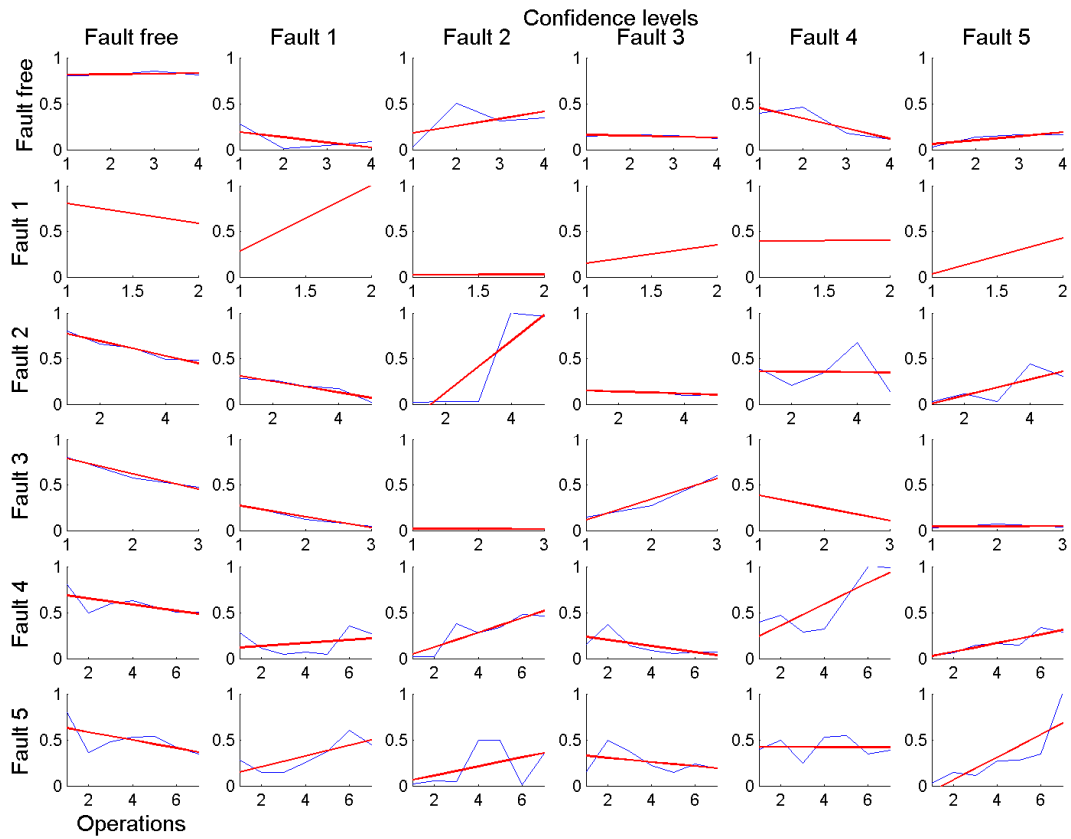


**Figure 20 - Output of the fault diagnosis algorithm for right to left throws**



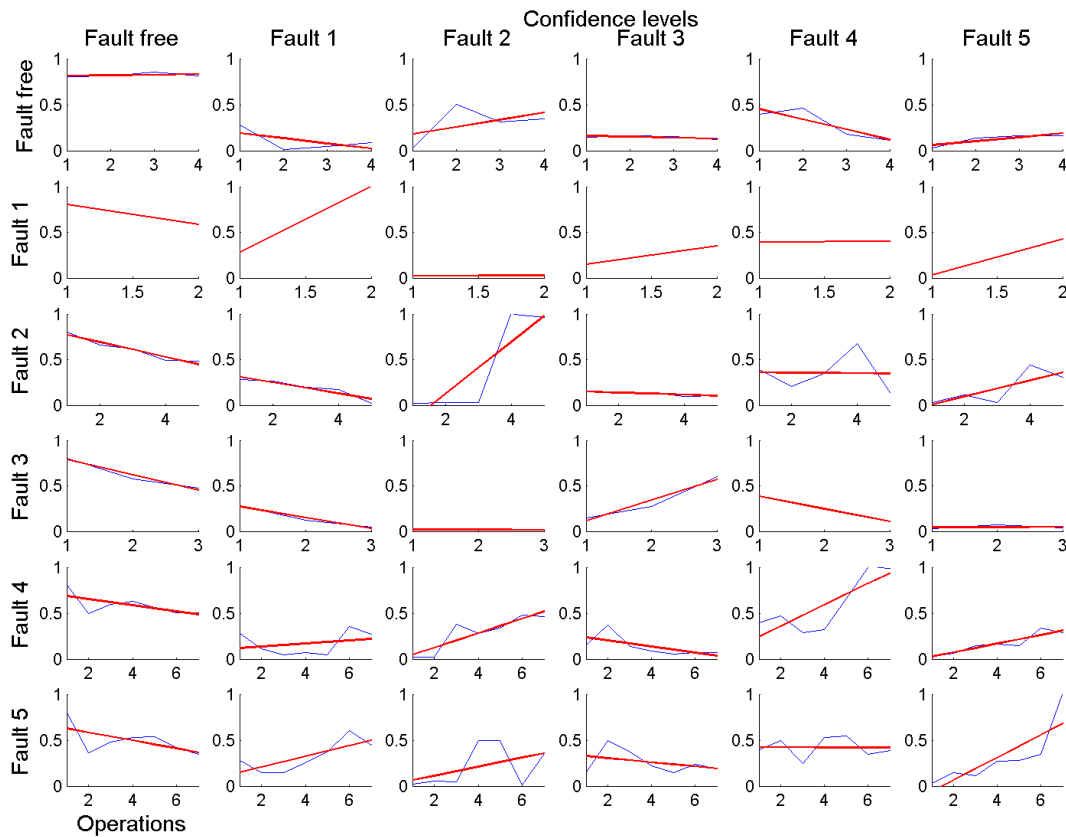


Figure 20 and Figure 21 show the output of the fault diagnosis algorithm for the data gathered at Berlin Ostbahnhof. The directions of operation are right-to-left and left-to-right respectively. The format of these graphs is identical to that of Figure 19: the rows are the confidence graphs for a particular fault simulation. Table 2 provides a description for the numbered faults in the graphs.

Fault number	Description
1	Left-hand locking mechanism tightened
2	Left-hand locking mechanism loosened
3	Right-hand locking mechanism tightened
4	Right-hand locking mechanism loosened
5	Fulcrum point brought closer to actuator

**Table 2 - Fault descriptions**

As with the ideal graphs, these real results show a strong response by the system to a fault being introduced: all the graphs along the diagonal have a strong positive trend. In each case, the gradient of the trend for the fault being simulated is greater than the gradient of any other trend.

Faults 1 and 5 appear to correlate quite closely. This suggests that the symptoms of these faults are quite similar, although one is a different scale to the other. The use of variable gradients in the membership functions has allowed rules to be created for each of these faults separately, despite the effects being quite similar. The symptom of each of these faults is an increase in the force towards the end of the throw, so it is not surprising that they correlate well.

These results are promising but they do not tell the full story. In order to be completely satisfactory, more data would need to be obtained, from another S700K switch, so that the rules could be used in their full

capacity on an actuator which was not used for the fault simulations. This would prove that it is possible to establish rules on only one instance of an actuator, and apply them across a wide asset base of similar actuators, which could number in the thousands.

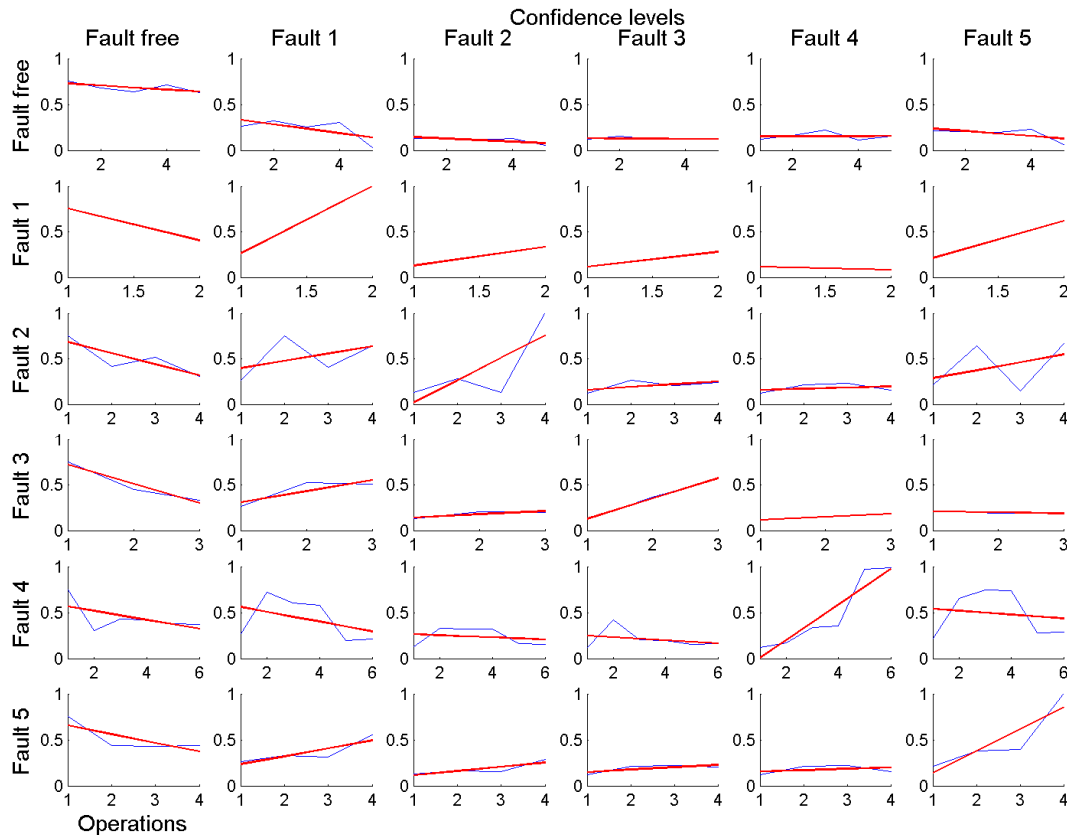


**Figure 21 - Output of the fault diagnosis algorithm for left to right throws**

## 5.7 Achieving a practical solution

It should be noted that this algorithm is not, in its present state, a practical solution for condition monitoring. There are certain problems which need to be overcome, not least of which is the weak point in the method: the use of differences between fault free and measured values to evaluate fault memberships. This method works best when the actuator used to create the rules is of a similar size and condition to the monitored actuator.

One solution to this might be to categorise switches of differing lengths as individual “actuator” types – establishing rules independently on each. Since switches of varying lengths exist in training schools, this is not an impossible solution. However, it does not address the problem completely.

The key, then, is to find a more effective way of achieving a value for “relative performance” which translates better between different instances of an actuator. However, the results presented here show that the qualitative trend analysis approach is effective as a framework for a more intelligent monitoring system.

Another point to note is that this algorithm ought to be used as one part of an integrated, larger system which takes advantage of the capabilities of monitoring approaches already in use. Some faults can be detected with very simple systems and there is no need to then overlay this algorithm on those faults, unless it can be demonstrated that it is more accurate or effective.

## 6. Conclusions

---

This report has presented the results of in-depth research into switch actuator condition monitoring. It is fair to conclude that there are dozens, if not hundreds, of perfectly valid advanced methods which can be used to diagnose the condition of a switch actuator, but most of them result in requirements such as large amounts of data, intensive mathematical modelling or a very advanced understanding on the part of the user. This does not mean that they cannot be used, however, and it is certain that elements of the complex methods reviewed in this report can and should be evaluated for further use. This is especially true of centralised condition monitoring systems, where data are collected at the switch site but then sent to a server to be analysed centrally. Here, complex algorithms and the attentions of highly-qualified staff are not impractical to implement.

However, this report also presents a possible solution which is based wholly on the requirements of the rail industry: for a system which requires minimal input data and analyses it in a similar fashion to how a human would – making it easier for technicians to understand the output.

There remains much work to be done in this field. So far, railway condition monitoring manufacturers have focused on providing simple, robust systems for field deployment. Effort now should be directed towards taking concepts such as the one presented here and developing them into practical solutions which can be implemented on the railway. This does not negate the work done towards providing the simple equipment – with some careful design, the complex analysis should be able to run as an extra layer to the capability which has already been provided.

# Appendix A Graphs of data collected at Berlin Ostbahnhof

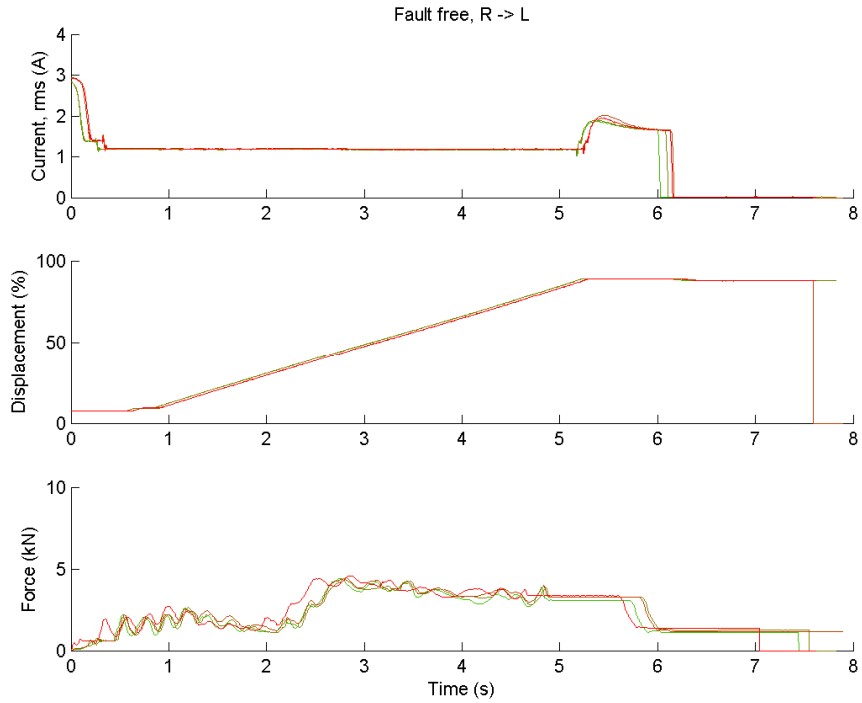


**Figure 22 - Fault free data, throwing right to left**

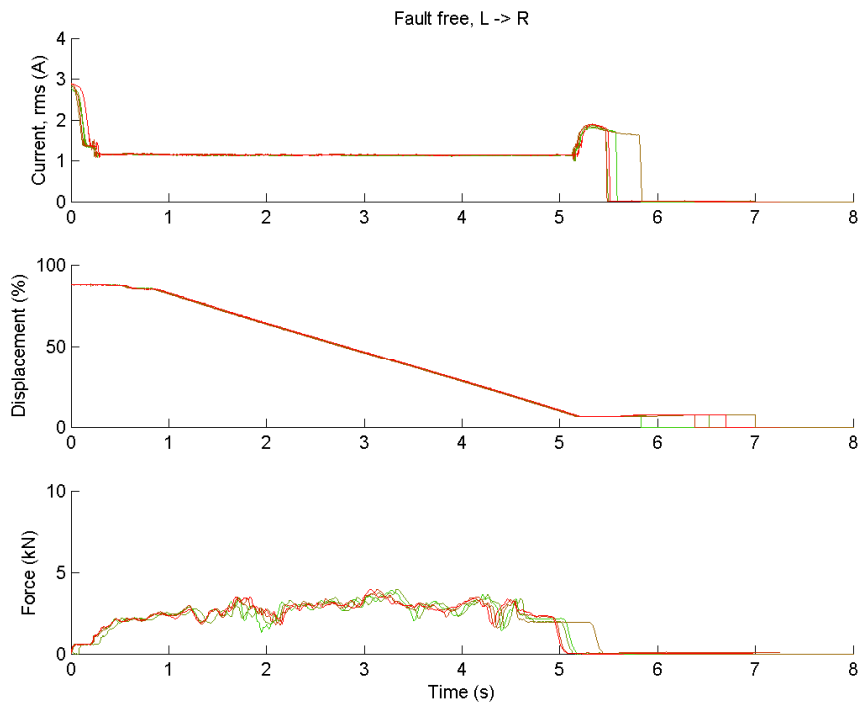


**Figure 23 - Fault free data, throwing left to right**

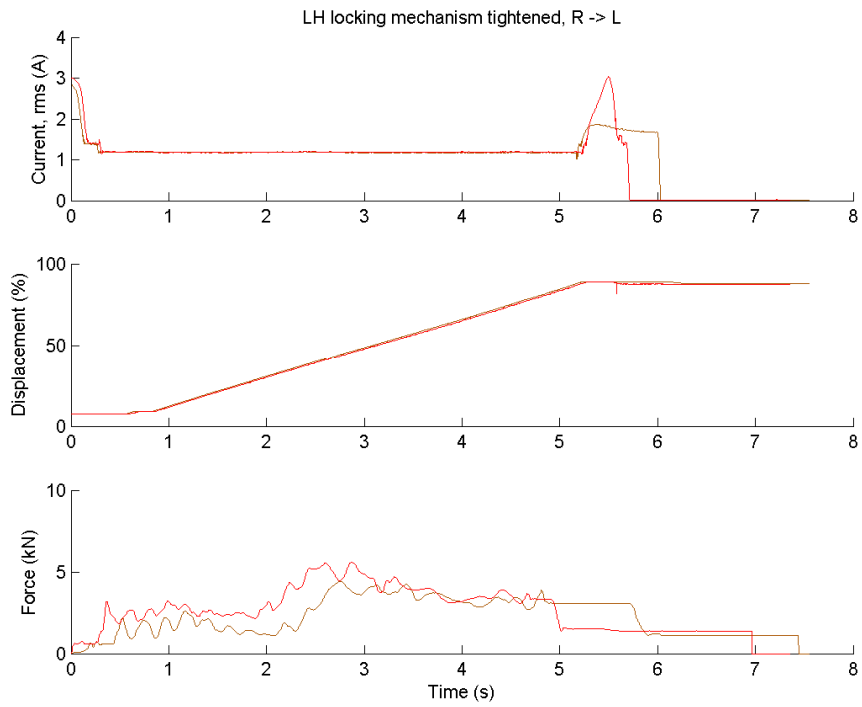


**Figure 24 - left hand locking mechanism tightened, throwing right to left**

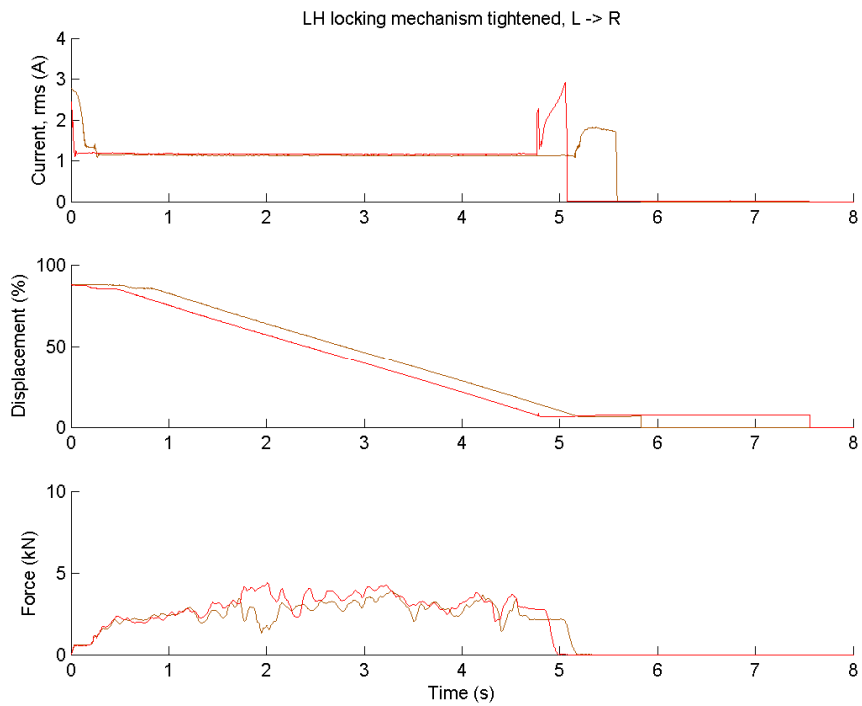


**Figure 25 - left hand locking mechanism tightened, throwing left to right**

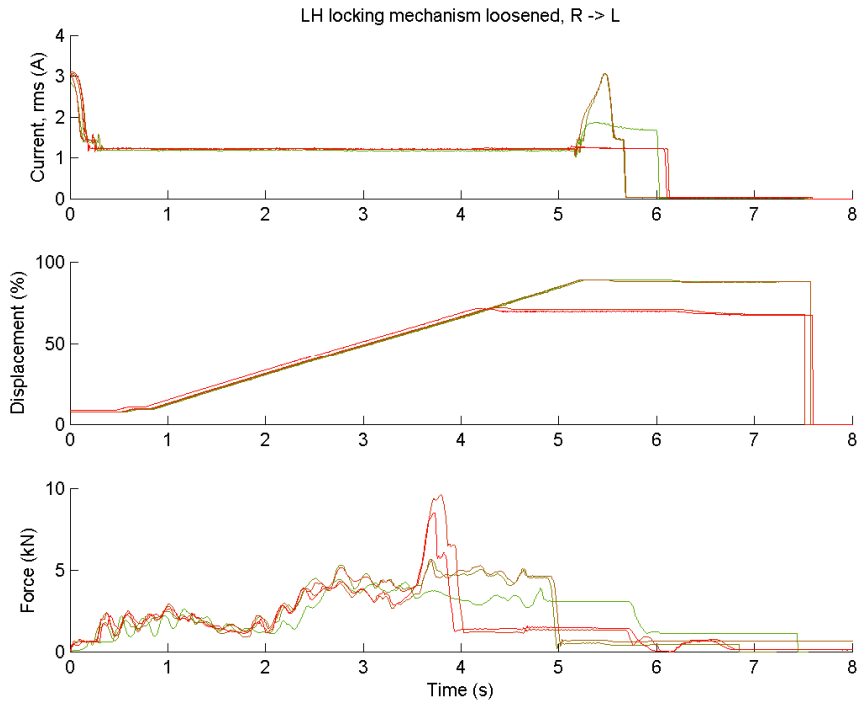


**Figure 26 - left hand locking mechanism loosened, throwing right to left**

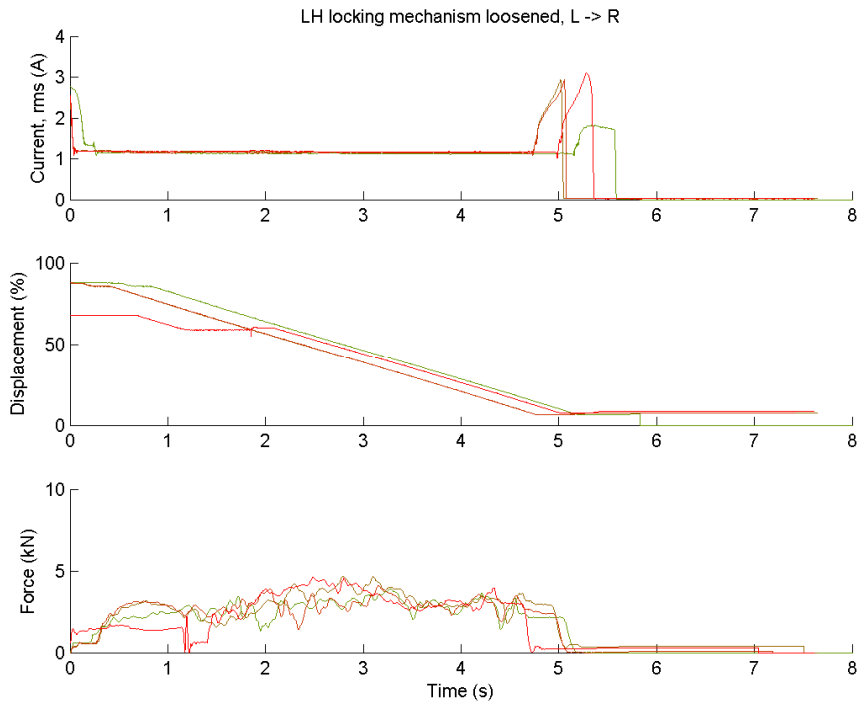


**Figure 27 - left hand locking mechanism loosened, throwing left to right**

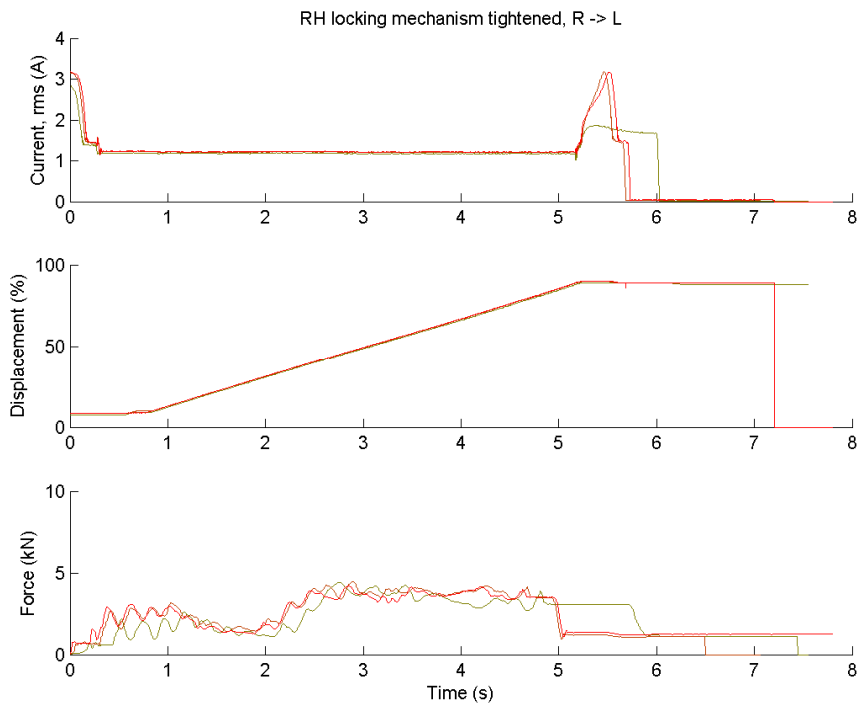


**Figure 28 - right hand locking mechanism tightened, throwing right to left**

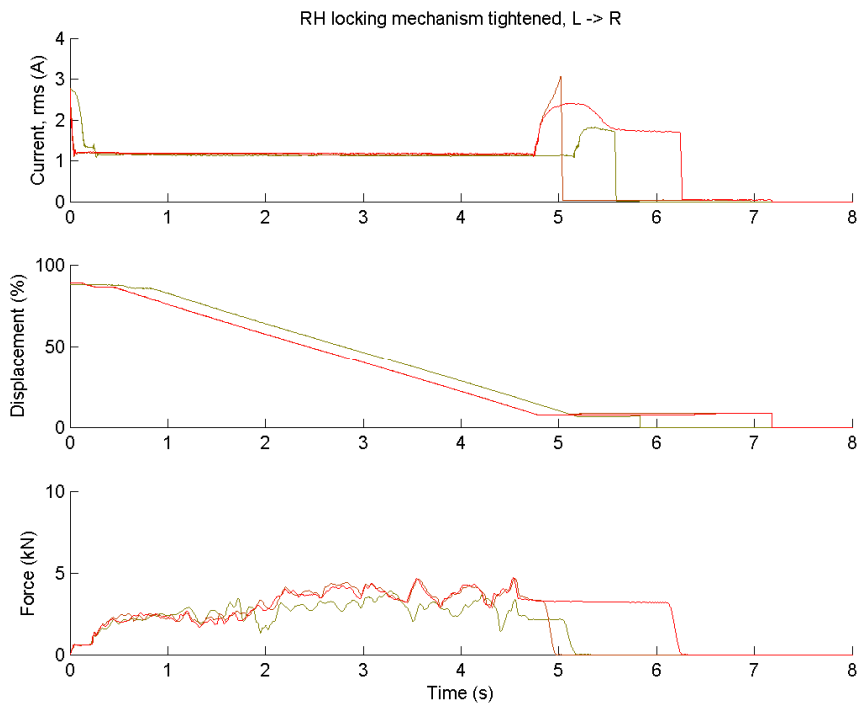


**Figure 29 - right hand locking mechanism tightened, throwing left to right**

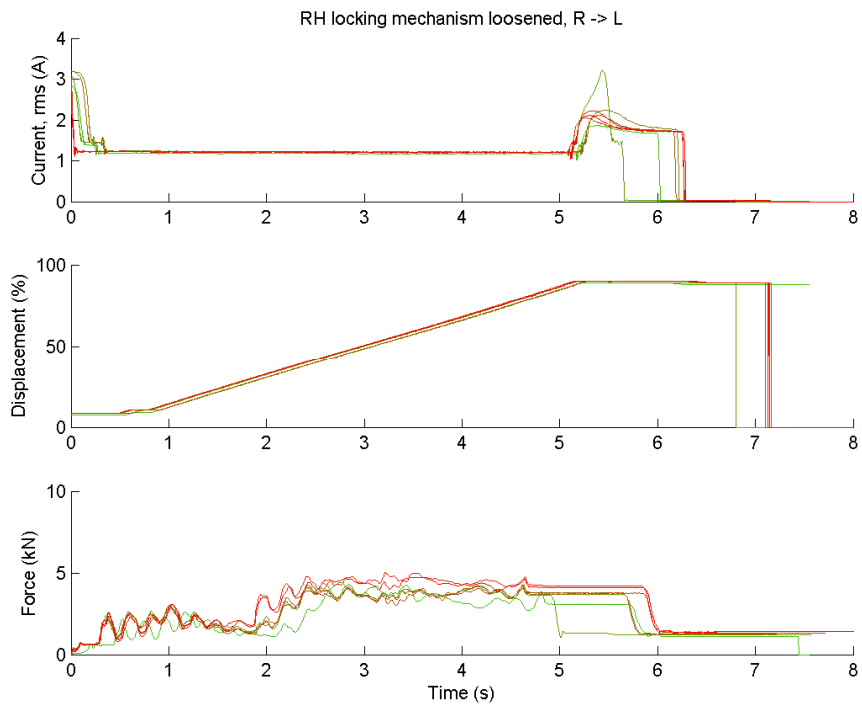


**Figure 30 - right hand locking mechanism loosened, throwing right to left**

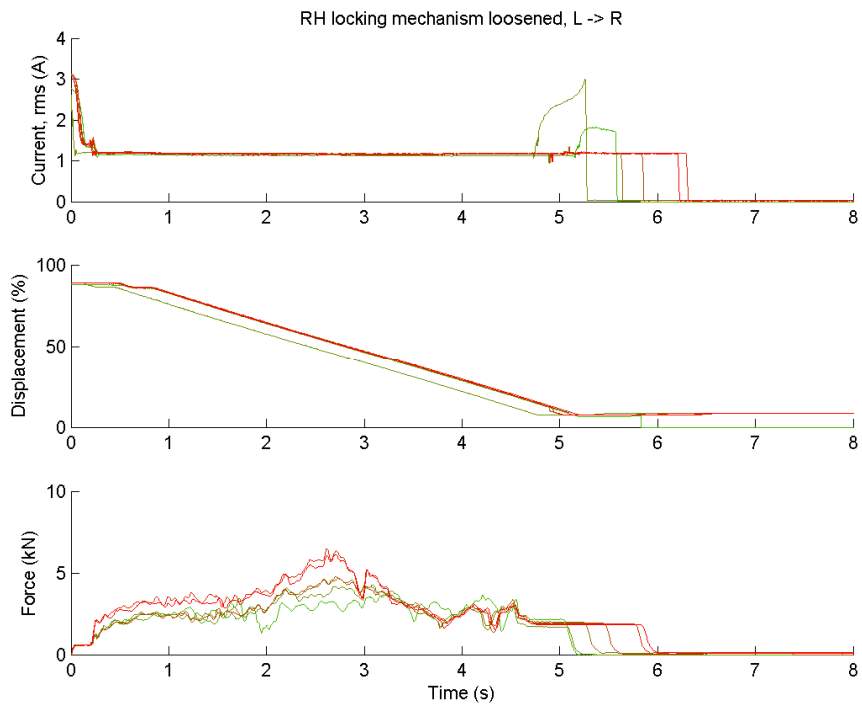


**Figure 31 - right hand locking mechanism loosened, throwing left to right**



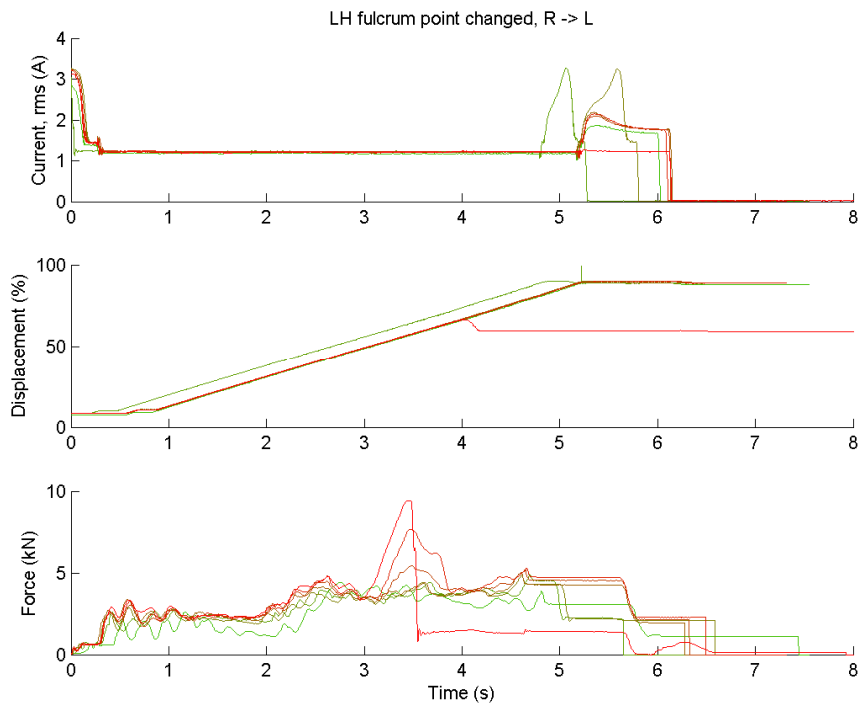


**Figure 32 - left hand fulcrum point changed, throwing right to left**

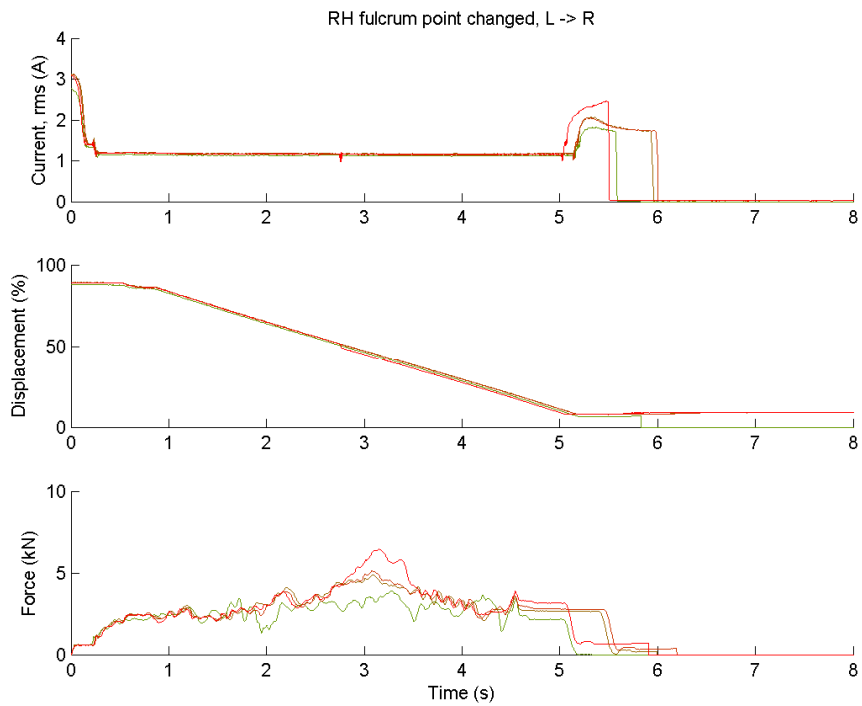


**Figure 33 - right hand fulcrum point changed, throwing left to right**

## References

---

1. *A review of process fault detection and diagnosis; Part I: Quantitative model-based methods.* **Venkatasubramanian, Venkat, et al.** s.l. : Elsevier, 2003, Computers & Chemical Engineering, Vol. 27, pp. 293-311.
2. *Application of a model-based fault detection and diagnosis using parameter estimation and fuzzy inference to a DC servomotor.* **Abidin, M Shukri Zainal, et al.** 2002. Proceedings of the 2002 IEEE International Symposium on Intelligent Control. pp. 783-788.
3. *A robustness study of model-based fault diagnosis for jet engine systems.* **Patton, Ron and Chen, J.** 1992. Proceedings of 1st IEEE Conference on Control Applications. pp. 871-876.
4. *Fault detection and diagnosis in turbine engines using fuzzy logic.* **Gayme, Dennice, et al.** 2003. NAFIPS 2003: 22nd International Conference of the North American Fuzzy Information Processing Society. pp. 341-346.
5. *Fault diagnosis in dynamic systems using analytical and knowledge-based redundancy: a survey and some new results.* **Frank, Paul M.** 3, 1990, Automatica, Vol. 26, pp. 459-474.
6. *Fault detection based on adaptive parity equations and single parameter tracking.* **Höfling, T and Isermann, Rolf.** 10, 1996, Control Engineering Practice, Vol. 4, pp. 1361-1369.
7. *Generating directional residuals with dynamic parity relations.* **Gertler, Janos J and Monajemy, Ramin.** 4, 1995, Automatica, Vol. 31, pp. 627-635.
8. *The dedicated observer approach to instrument failure detection.* **Clark, R N.** 1979. Proceedings of the 18th IEEE Conference on Decision and Control inc. the Symposium on Adaptive Processes. Vol. 18, pp. 237-241.
9. *Closed-loop fault diagnosis based on a nonlinear process model and automatic fuzzy rule generation.* **Ballé, Peter and Füssel, Dominik.** 2000, Engineering Applications of Artificial Intelligence, Vol. 13, pp. 695-704.
10. *Incipient fault diagnosis of dynamical systems using online approximators.* **Demetriou, Michael A and Polycarpou, Marios M.** 11, 1998, IEEE Transactions on Automatic Control, Vol. 43, pp. 1612-1617.
11. **Travé-Massuyès, Louise and Milne, Robert.** Gas-turbine condition monitoring using qualitative model-based diagnostics. *IEEE Expert.* 1997, pp. 22-31.
12. *Qualitative modelling of continuous-variable systems by means of non-deterministic automata.* **Lunze, Jan.** 1, 1992, Intelligent Systems Engineering, Vol. 1, pp. 22-30.
13. *Observation of qualitative states by means of a qualitative model.* **Lichtenberg, G and Lunze, Jan.** 6, 1997, International Journal of Control, Vol. 66, pp. 885-903.
14. *Diagnosis of transient faults in quantised systems.* **Schiller, Frank, Schröder, Jochen and Lunze, Jan.** 2001, Engineering Applications of Artificial Intelligence, Vol. 14, pp. 519-536.
15. *Deterministic discrete-event representations of linear continuous-variable systems.* **Lunze, Jan, Nixdorf, B and Schröder, Jochen.** 199, Automatica, Vol. 35, pp. 395-406.
16. *Diagnosis of quantized systems based on a timed discrete-event model.* **Lunze, Jan.** 3, 2000, IEEE Transactions on Systems, Man and Cybernetics, Vol. 30.
17. *Structured fault-detection and diagnosis using finite state-automaton.* **Ramkumar, K B, et al.** 1998. Proceedings of the 24th Annual Conference of the IEEE Industrial Electronics Society. Vol. 3, pp. 1667-1672.
18. *An algorithm for diagnosis of system failures in the chemical process.* **Iri, M, et al.** 1979, Computers and Chemical Engineering, Vol. 3, pp. 489-493.
19. *Fault diagnosis, direct graphs, and fuzzy logic.* **Tarifa, Enrique A and Scenna, Nicolás J.** 1997, Computers and Chemical Engineering, Vol. 21, pp. S649-S654.
20. **Forbus, Kenneth D.** Qualitative physics: past, present and future. *Exploring artificial intelligence.* s.l. : Morgan Kaufmann Publishers Inc., 1988, 7, pp. 239-296.
21. *A qualitative physics based on confluences.* **de Kleer, J and Brown, J S.** 1984, Artificial Intelligence, Vol. 24, pp. 7-83.

22. *On-line hazard aversion and fault diagnosis in chemical processes: the digraph + fault tree method.* **Ulerich, Nancy H and Powers, Gary J.** 2, 1988, IEEE Transactions on Reliability, Vol. 37, pp. 171-177.
23. *A review of process fault detection and diagnosis, part II: Qualitative model-based methods.* **Venkatasubramanian, Venkat, Rengaswamy, Raghunathan and Kavuri, Surya N.** 2003, Computers and Chemical Engineering, Vol. 27, pp. 313-326.
24. *Narrowing diagnostic focus using functional decomposition.* **Finch, F E and Kramer, M A.** 1, 1988, AIChE Journal, Vol. 34, pp. 25-36.
25. *A review of process fault detection and diagnosis, part III: Process history based methods.* **Venkatasubramanian, Venkat, et al.** 2003, Computers and Chemical Engineering, Vol. 27, pp. 327-346.
26. *Face recognition using kernel Principal Component Analysis.* **Kim, Kwang In, Jung, Keechul and Kim, Hang Joon.** 2, 2002, IEEE Signal Processing Letters, Vol. 9, pp. 40-42.
27. *Two-dimensional PCA: A new approach to appearance based face representation and recognition.* **Yang, Jian, et al.** 1, 2004, IEEE Transactions on Pattern Analysis and Machine Intelligence, Vol. 26, pp. 131-137.
28. *A feature extraction technique based on Principal Component Analysis for pulsed eddy current NDT.* **Sophian, Ali, et al.** 2003, NDT&E International, Vol. 36, pp. 37-41.
29. *Prediction of spalling on a ball bearing by applying the discrete wavelet transform to vibration signals.* **Mori, K, et al.** 1996, Wear, Vol. 195, pp. 162-168.
30. *Cluster-based feature extraction and data fusion in the wavelet domain.* **Sveinsson, Johannes R, Ulfarsson, Magnus Orn and Benediktsson, Jon Atli.** 2001. IEEE International Geoscience and Remote Sensing Symposium. Vol. 2, pp. 867-869.
31. *Optimising the application of the Hough transform for automatic feature extraction from geoscientific images.* **Fitton, N C and Cox, S J D.** 10, 1998, Computers & Geosciences, Vol. 24, pp. 933-951.
32. *Fuzzy wavelet packet based feature extraction method and its application to biomedical signal classification.* **Li, Dequiang, Pedrycz, Witold and Pizzi, Nicolino J.** 6, 2005, IEEE Transactions on Biomedical Engineering, Vol. 52, pp. 1132-1139.
33. *Feature extraction from wavelet coefficients for pattern recognition tasks.* **Pittner, Stefan and Kamarthi, Sagar V.** 1, 1999, IEEE Transactions on Pattern Analysis and Machine Intelligence, Vol. 21, pp. 83-88.
34. *Wavelet packet feature extraction for vibration monitoring.* **Yen, Gary G and Lin, Kou-Chung.** 3, 2000, IEEE Transactions on Industrial Electronics, Vol. 47, pp. 650-667.
35. *Artificial neural networks: fundamentals, computing, design and application.* **Basheer, I A and Hajmeer, M.** 2000, Journal of Microbiological Methods, Vol. 43, pp. 3-31.
36. *Condition assessment of power transformers using genetic-based neural networks.* **Huang, Y-C.** 1, 2003, IEE Proceedings on Science, Measurement and Technology, Vol. 150, pp. 19-24.
37. *Neural network based fault detection in robotic manipulators.* **Vemuri, A T, Polykarpou, M M and Diakourtis, S A.** 2, 1998, IEEE Transactions on Robotics and Automation, Vol. 14.
38. *Representation of process trends - Part I: A formal representation framework.* **Cheung, J T-Y and Stephanopoulos, G.** 4/5, 1990, Computers and Chemical Engineering, Vol. 14, pp. 495-510.
39. *Representation of process trends - Part II: The problem of scale and qualitative scaling.* **Cheung, J T-Y and Stephanopoulos, G.** 4/5, 1990, Computers and Chemical Engineering, Vol. 14, pp. 511-539.
40. *Representation of process trends - Part III: Multiscale extraction of trends from process data.* **Bakshi, B R and Stephanopoulos, G.** 4, 1994, Computers and Chemical Engineering, Vol. 18, pp. 267-302.
41. *Representation of process trends - Part IV: Induction of real-time patterns from operating data for diagnosis and supervisory control.* **Bakshi, B R and Stephanopoulos, G.** 4, 1994, Computers and Chemical Engineering, Vol. 18, pp. 303-332.
42. *A systems approach to fault detection and diagnosis for condition-based maintenance.* **Silmon-Monerri, Joseph Alan and Roberts, Clive.** 2006. Proceedings of the 1st IET International Conference on Railway Condition Monitoring.
43. *SQFDiag: Semiquantitative model-based fault monitoring and diagnosis via episodic fuzzy rules.* **Özyurt, Ibrahim Burak, Hall, Lawrence O and Sunol, Aydin K.** 3, 1999, IEEE Transactions on Systems, Man and Cybernetics - Part A: Systems and Humans, Vol. 29, pp. 294-306.

44. *An expert system for transformer fault diagnosis using dissolved gas analysis.* **Lin, C E, Ling, J M and Huang, C L.** 1, 2003, IEEE Transactions on Power Delivery, Vol. 8, pp. 231-238.
45. *An expert system-based framework for an incipient failure detection and predictive maintenance system.* **Butler, Karen L.** 1996. Proceedings of the International Conference on Intelligent Systems Applications to Power Systems. pp. 321-326.
46. *An integrated neural network/expert system approach for fault diagnosis.* **Becraft, W R and Lee, P L.** 10, 1993, Computers and Chemical Engineering, Vol. 17, pp. 1001-1014.
47. *A combined ANN and expert system tool for transformer fault diagnosis.* **Wang, Zhenyuan, Liu, Yilu and Griffin, Paul J.** 4, 1998, IEEE Transactions on Power Delivery, Vol. 13, pp. 1224-1229.
48. **Advantage Technical Consulting.** *Review of the reliability of point motors and track circuits.* 2002. 25017-04-rep-01.
49. *Remote condition monitoring for railway point machine.* **Zhou, F B, Duta, M D and Henry, M P.** 2002. Proceedings of the ASME/IEEE Joint Rail Conference. pp. 103-108.
50. *Distributed quantitative and qualitative fault diagnosis: railway junction case study.* **Roberts, Clive, et al.** 2002, Control Engineering Practice, Vol. 10, pp. 419-429.
51. *Industrial fault diagnosis: pneumatic train door case study.* **Lehrasab, Nadeem, et al.** 2002, Proceedings of the IMechE, Part F: Rail and Rapid Transit.
52. *Introduction to the DAMADICS actuator FDI benchmark study.* **Bartyś, Michal, et al.** 2006, Control Engineering Practice, Vol. 14, pp. 577-596.
53. **Syfert, Michal.** DAMADICS RTN Information Website. [Online] 2002. [Cited: 24 3 2009.] <http://diag.mchtr.pw.edu.pl/damadics/>.
54. *FDI approach to the DAMADICS benchmark problem based on qualitative reasoning coupled with fuzzy neural networks.* **Calado, J M F, et al.** 2006, Control Engineering Practice, Vol. 14, pp. 684-698.
55. *Diagnosis of timed automata: Theory and application to the DAMADICS actuator benchmark problem.* **Supavatanakul, P, et al.** 2006, Control Engineering Practice, Vol. 14, pp. 609-619.
56. *Passive robust fault detection using interval observers: Application to the DAMADICS benchmark problem.* **Puig, V, et al.** 2006, Control Engineering Practice, Vol. 14, pp. 621-633.
57. *A GMDH neural network-based approach to robust fault diagnosis: Application to the DAMADICS benchmark problem.* **Witczak, Marcin, et al.** 2006, Control Engineering Practice, Vol. 14, pp. 671-683.
58. *Model-free actuator fault detection using a spectral estimation approach: the case of the DAMADICS benchmark problem.* **Previdi, F and Parisini, T.** 2006, Control Engineering Practice, Vol. 14, pp. 635-644.
59. *Application of a novel fuzzy classifier to fault detection and isolation of the DAMADICS benchmark problem.* **Bocaniala, Cosmin Danut and Sá da Costa, Jose.** 2006, Control Engineering Practice, Vol. 14, pp. 653-669.
60. *Identification of discrete event models for continuous-variable systems.* **Lichtenberg, G and Lunze, Jan.** 1996. Proceedings of the UKACC International Conference on Control. Vol. 1, pp. 711-715.